

**Hyperthermal rare-gas ion-stimulated CN<sup>-</sup> desorption from a nitrogenated graphite surface**

Z.-W. Deng\* and R. Souda†

*Advanced Materials Laboratory, National Institute for Materials Science (AML/NIMS) 1-1 Namiki, Tsukuba, Ibaraki 305, Japan*

(Received 17 September 2002; revised 22 January 2003; published 6 June 2003)

The mechanism of hyperthermal (2–30 eV) rare-gas (*RG*) ions induced CN<sup>-</sup> desorption from a nitrogenated graphite surface is investigated. CN<sup>-</sup> desorption occurs at an incident energy as low as 2 eV and gains a relatively high energy from the desorption process in comparison with the incident kinetic energy. A strong correlation is observed between the CN<sup>-</sup> maximum translational energy (MTE) and the incident *RG* ion energy, suggesting a localized interaction between the incident ion and surface CN species. A MTE of ~5 eV is obtained at 0-eV incident energy, and is found independently of the incident ion species. It is proposed that CN<sup>-</sup> emission occurs as a result of the potential desorption of chemisorbed surface CN species mediated by the formation of a localized hole at its bonding or nonbonding orbital via (quasi)resonant neutralization of an incident *RG* ion.

DOI: 10.1103/PhysRevB.67.235402

PACS number(s): 79.20.Rf, 34.50.Gb, 34.70.+e

**I. INTRODUCTION**

Desorption induced by electron transition (DIET) has been a research subject of great interest and importance in both pure science and practical applications for over four decades. In this respect, electron- and photon-stimulated desorptions (ESD, PSD) have been extensively investigated and many fundamental processes have been revealed. This is manifested by the mechanisms proposed to account for the desorption dynamics.<sup>1</sup> In ESD and PSD, the incident electron or photon induces a Franck-Condon transition between the ground and the excited states of a system, subsequent decay of the excited state converts the potential energy to the translational energy of the ejected particle (the Menzel-Gomer-Redhead (MGR) model<sup>2,3</sup>). Knotek and Feibelman<sup>4</sup> also proposed a different mechanism (KF model) to account for the positive ion desorption from some ionic surfaces, in which the negative ion in the ionic solid is turned into a positive ion as a result of intra-atomic or interatomic Auger decay of a core hole produced by the photon or electron irradiation. This idea (also termed Auger desorption, AD) has also been generalized to covalent materials or chemisorption systems on metals,<sup>5</sup> in which the local Coulomb interaction and the correlation effect of the holes may play an important role.<sup>6–9</sup>

Since any ionizing irradiation can initiate DIET, the ion-beam induced potential emission of secondary ions from surface has recently attracted considerable attention.<sup>10–23</sup> During ion-surface interaction, the incident ions are neutralized in most cases via resonant or Auger charge transfer processes with the surface. The subsequent surface chemical reaction is thus believed to be stimulated by the translational energy carried by the incident ion.<sup>24,25</sup> Nevertheless, the role of the potential energy carried by the incident ion (or in other words, the hole of the incident ion) has been suspected for a long time to play a considerable role in stimulating chemical reactions.<sup>10–15</sup> Very recently, it has been demonstrated that the hole of an incident ion or even an excited atom can play a dominant role in stimulating surface desorption in some specific cases.<sup>16–22,26</sup> By decreasing the incident ion energy to the hyperthermal level (several to tens of electron volts), the collision effect can be neglected or distinguished, facili-

tating the observation of chemical and electronic effects on surface reactions and desorptions.<sup>24–27</sup>

In this paper, we report that hyperthermal (2–30 eV) rare-gas (*RG*) ions induce CN<sup>-</sup> desorption from a nitrogenated graphite surface. Basing on a correlation between the product maximum translational energy and the incident ion energy, we demonstrate that the CN<sup>-</sup> emission occurs as a result of potential-stimulated desorption. Briefly, localized resonant or quasi-resonant decay of the incident ion's hole by an electron from a bonding or nonbonding molecular orbital of chemisorbed CN species creates a localized hole at the molecular orbital. Subsequent decay of the excited state imparts kinetic energy to the surface CN and results in ejection of CN species from the surface. The desorbing CN species then capture electrons from the surface via resonant process during departure, yielding CN<sup>-</sup> ions.

**II. EXPERIMENT**

The experiments were carried out in a ultrahigh vacuum (UHV) system with a base pressure of  $<1 \times 10^{-10}$  Torr, which combines a mass-separated low-energy ion beam system and an energy-resolved quadrupole mass spectrometer. The system has been described elsewhere.<sup>28</sup> The low-energy ion beam system can deliver an ion beam with an energy of 2–800 eV. In this work, it was first used to produce a 500-eV N<sub>2</sub><sup>+</sup> ion beam to implant nitrogen into a pyrolytic graphite sample surface. Briefly, nitrogen plasma was produced via electron impact in a hot filament ion source. Positive ions were extracted from an anode hole with a –20-kV bias, and transported at this voltage to a 90° magnetic sector for mass selection, where the N<sub>2</sub><sup>+</sup> ions were permitted to pass through, while ions with other mass/charge ratios were filtered and neutrals were also eliminated from the beam line thereafter. The N<sub>2</sub><sup>+</sup> ions were subsequently focused and finally decelerated to 500 eV for implantation. The ion source was positively biased with respect to the target maintained at earth potential, which determined the incident ion energy.

The graphite sample was cleaved in air and further cleaned in UHV by heating via electron bombardment up to 1200 °C for several cycles. After cooling down to room tem-

perature, it was irradiated by 500-eV  $N_2^+$  ions with a dose of  $\sim 10^{18}$  ions/cm<sup>2</sup>, which resulted in the formation of a carbon nitride film at graphite surface. The film has been investigated previously.<sup>29,30</sup> The results show that the carbon nitride film mainly consists of single and double C—N bonds.<sup>29</sup> Heating of the film leads to the desorption of  $N_2$ ,  $C_2N_2$  molecules and  $CN^-$  ions.<sup>29,30</sup> At the top surface, there exist chemisorbed (weak-bound) cyanogen (CN) molecules, which was demonstrated indirectly by its enhancement effect on sputtering of  $C^+$  ions from graphite surface.<sup>28</sup> The chemisorbed CN is believed to be the precursor of  $CN^-$  desorption as observed later in this work.

After nitrogen implantation, the ion beam system was used to produce rare-gas ions, and the nitrogenated graphite surface was then subjected to 2–30-eV  $Ar^+$ ,  $Ne^+$ , or  $He^+$  irradiation, during which  $CN^-$  ion emission was observed. An incident ion current density of 0.5–1.5  $\mu A/cm^2$  with an energy of 2–30 eV was readily obtained. The energy spread of the ion beam was determined to be within 2 eV in this energy range. The  $CN^-$  yield and energy distribution were recorded as a function of the incident ion energy under a specular scattering profile. During experiments, background was measured with the sample moved out of the way and subtracted from the ion yields presented in this work.

The mass spectrometer, mounted at an angle of 70° with respect to the ion beam line, consists of a high-transmission 45° sector field energy analyzer and a quadrupole mass spectrometer.<sup>28</sup> It allows for measuring the energy and the mass distribution of secondary ions. The ion energy is analyzed by the field energy analyzer at a constant pass energy by scanning a filter voltage, and the ion mass is analyzed by the rf quadrupole. The energy resolution of the analyzer is estimated to be  $\sim 1.2$  eV in full width at half maximum from the thermionic ion distribution.

### III. EXPERIMENTAL RESULTS

Figure 1 presents typical incident energy dependence of integrated  $CN^-$  yield produced by 2–30-eV  $Ar^+$ ,  $Ne^+$ , and  $He^+$  irradiation of a nitrogenated graphite surface. The ion yield has been normalized by the incident ion current. As a comparison, the energy dependence of  $CN^-$  yield produced by hyperthermal  $N^+$  abstraction of carbon from graphite is also presented (labeled  $N^+$ ), which yields an incident energy threshold of  $\sim 0$  eV for  $CN^-$  emission.<sup>27</sup> During  $RG$  ion irradiation, the kinetic effect emerges at an incident energy of  $\sim 10$  eV. Below 10 eV, the change of the  $CN^-$  yield is insignificant, which will be demonstrated in this work to be a result of potential desorption. The kinetic effect is ascribed to collision-enhanced potential desorption and/or kinetic sputtering. Note that the  $CN^-$  yield is also dependent on the incident  $RG$  ion species in an order of  $Ar^+ > Ne^+ > He^+$ .

The above results suggest a facile emission of  $CN^-$  ions that is also demonstrated by the high translational energy available to the  $CN^-$  ions. Figure 2(a) presents normalized translational energy distributions of  $CN^-$  ions produced by 2-eV  $Ar^+$ ,  $Ne^+$ , and  $He^+$  irradiation of a nitrogenated graphite surface. The translational-energy scale has been calibrated by thermionic  $CN^-$  ions. The ordinate is broken to

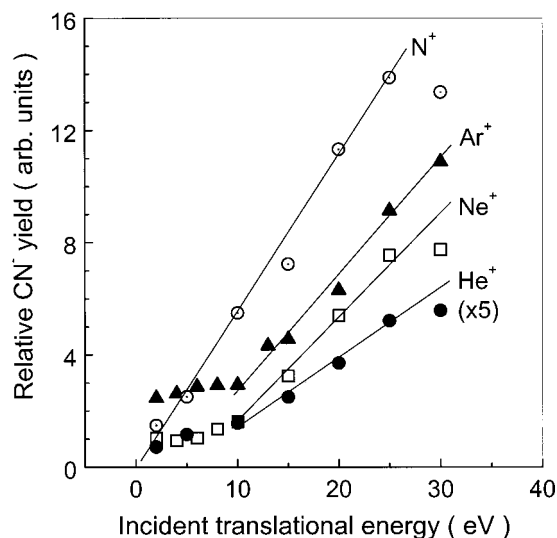


FIG. 1. Integrated  $CN^-$  yield as a function of incident energy during 2–30-eV  $Ar^+$ ,  $Ne^+$ , and  $He^+$  ion irradiation of a nitrogenated graphite. Also shown as a comparison is the  $CN^-$  yield as a function of  $N^+$  energy produced by abstraction reaction. The lines are drawn to guide the eye.

show the cutoff positions of the high-energy tails of the  $CN^-$  distributions. The high-energy tail indicates the production of  $CN^-$  ions with an energy higher than the mean translational energy. Although, the amount is small, it is critical to account for the energy origin when tailoring the formation dynamics of  $CN^-$  ions as it may reflect a recoilless event.<sup>7,31</sup> As a comparison and reference, the energy distribution of the  $CN^-$  ions produced by a 2-eV  $N^+$  abstraction of carbon from graphite is also shown. The abstraction reaction has been demonstrated to occur at carbon defect sites and is exoergic by  $\sim 2$  eV, which, with the incident  $N^+$  kinetic energy, is partly converted into the product translational energy.<sup>27</sup> Then it is noted that both the mean and the maximum energies available to the  $CN^-$  ions produced by  $RG$  ion irradiation of a nitrogenated graphite surface are (much) higher than that produced by the abstraction reaction. Moreover, the  $CN^-$  maximum energies during  $Ar^+$ ,  $Ne^+$ , and  $He^+$  irradiation are very close, suggesting the independence of the incident ion species. With an increase in the incident  $RG$  ion energy, the high-energy tail exhibits a significant shift with the magnitude depending on the incident ion species, although the change of the mean translational energies are not that significant, as shown in Fig. 2(b).

Figure 3 shows the ion yield and energy distribution of the  $CN^-$  ions as a function of incident energy during 2–30-eV  $Ar^+$  irradiation, where the yield has been normalized by the incident ion current and the ordinate is broken to show the high-energy tails. The high-energy tail of the  $CN^-$  distribution exhibits a significant shift with the incident  $Ar^+$  energy. We will discuss the  $CN^-$  emission mechanism on the basis of the kinetic effect on the high-energy  $CN^-$  ions, which is characterized by the maximum translational energy (MTE) available to the product. The MTE is determined by extrapolating the high-energy tail to the zero signal after subtracting the background (noise), followed by correcting with

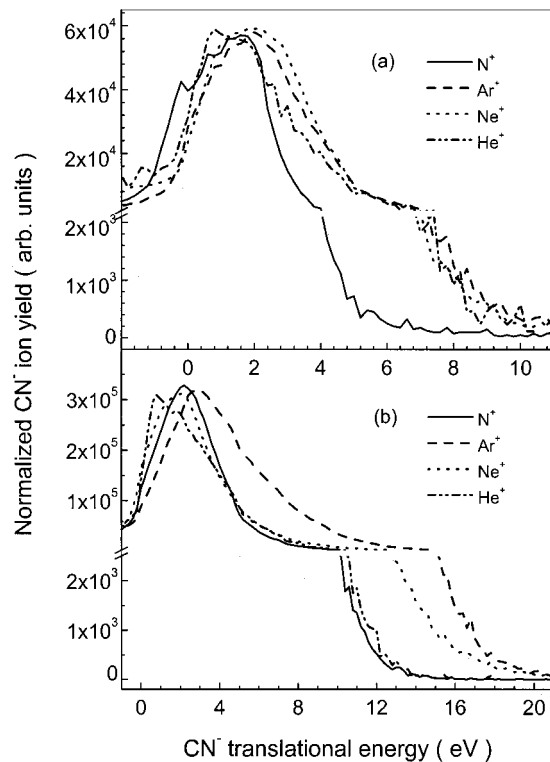


FIG. 2. Normalized translational energy distribution and cutoff position of the high-energy tail of CN<sup>-</sup> ions produced by (a) 2-eV and (b) 30-eV Ar<sup>+</sup>, Ne<sup>+</sup>, and He<sup>+</sup> ion irradiation of a nitrogenated graphite surface. Also shown by the solid line are the energy distribution and cutoff position of the high-energy tail of the CN<sup>-</sup> ions produced by (a) 2-eV and (b) 30-eV N<sup>+</sup> abstraction of carbon from graphite as a comparison and reference, which indicates that the high-energy tail of the CN<sup>-</sup> ions produced by RG ion irradiation is not due to instrumental factor(s) but demonstrates the formation of CN<sup>-</sup> ions with energy higher than that produced by N<sup>+</sup> abstraction reaction.

the thermionic CN<sup>-</sup> ions. It represents the maximum energy available to the CN<sup>-</sup> ion in its formation process. Figure 4 depicts the MTEs of CN<sup>-</sup> ions as obtained via the above method as a function of the incident Ar<sup>+</sup>, Ne<sup>+</sup>, and He<sup>+</sup> energies, as well as N<sup>+</sup> energy for comparison (resulting from abstraction reaction). The CN<sup>-</sup> MTE increases linearly with the incident ion energy, from which the maximum ratio of translational-energy transfer from incident ion to CN<sup>-</sup> product is obtained and depends on the incident ion species. By extrapolating the incident energy dependence, the CN<sup>-</sup> MTE under 0-eV RG ion irradiation is obtained as ~5 eV (without a collision effect). Then, it is remarkable to note that the CN<sup>-</sup> MTE obtained by 0-eV RG ion irradiation is (i) independent of the incident ion species, and (ii) much higher than that produced by 0-eV N<sup>+</sup> abstraction reaction (~1 eV). The possible CN<sup>-</sup> desorption dynamics will be discussed in light of the above results.

#### IV. DISCUSSION

The secondary ion or neutral desorption induced by energetic ion-surface interaction has been subjected to extensive

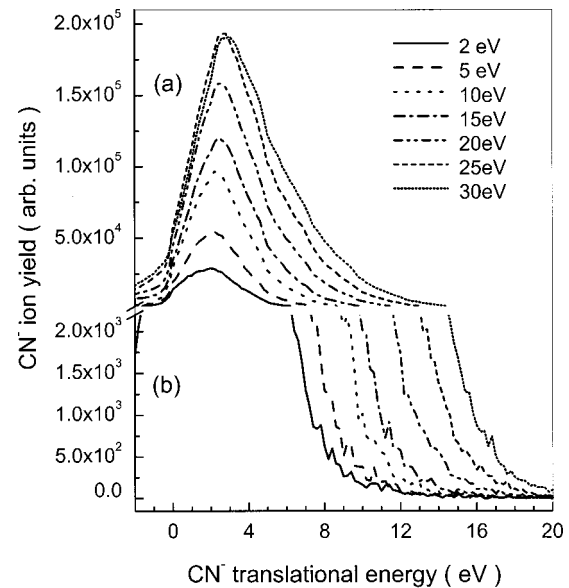


FIG. 3. (a) The yield and translational energy distribution of CN<sup>-</sup> ions produced by 2–30-eV Ar<sup>+</sup> ion irradiation of a nitrogenated graphite surface as a function of incident energy. The ordinate is broken to show the cutoff positions of the high-energy tails (b).

investigation in the past few decades. Most of the secondary particles are believed to be a result of kinetic sputtering process. In reality, however, the secondary particle emission can be a comprehensive result of both kinetic sputtering and electronic excitation. The latter has been employed to account for the noncollisional sputtering of O<sup>+</sup> and F<sup>+</sup> by rare-gas ion irradiation,<sup>11,15</sup> and is termed ion-stimulated de-

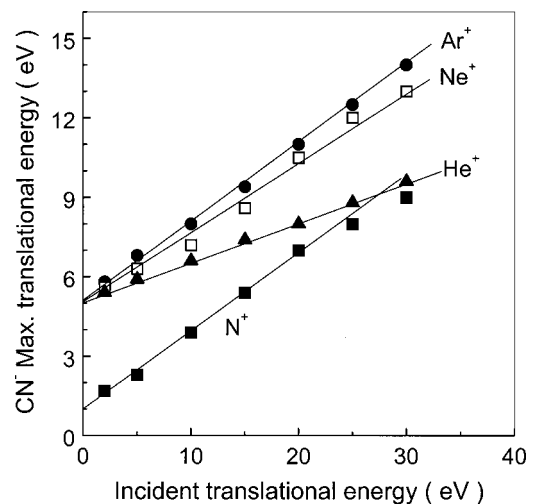


FIG. 4. The maximum translational energy (MTE) of CN<sup>-</sup> ions as a function of incident energy produced by 2–30-eV Ar<sup>+</sup>, Ne<sup>+</sup>, and He<sup>+</sup> ion irradiation of a nitrogenated graphite, as well as a hyperthermal N<sup>+</sup> abstraction of carbon from graphite (labeled N<sup>+</sup>). The lines are drawn to guide the eye. The results yield maximum translational-energy transfer ratios of ~30%, 26%, 14%, 25% for Ar<sup>+</sup>, Ne<sup>+</sup>, He<sup>+</sup>, and N<sup>+</sup> irradiation, respectively. Note the significant difference of CN<sup>-</sup> MTE produced by 0-eV RG ion irradiation and N<sup>+</sup> abstraction.

sorption (ISD). In this respect, the potential energy of the primary ion has been suspected to play an important role in initiating the desorption event. So far, several models have been proposed as possible dynamics of ISD. The creation of deep core holes by the impact of energetic primary ion leads to Auger electron emission that induces ESD as a subsidiary effect.<sup>11</sup> It is also possible that the Auger neutralization of the primary ion itself leads to secondary ion desorption, since two valence holes are created around the impact point.<sup>15</sup> These models are fundamentally in analogy with the ESD and PSD.<sup>10–15</sup>

While most studies on ESD, PSD, and ISD have focused on the nature of the initiating event, the lifetime of the excited state is also a critical prerequisite. Because the electronic dynamics as initiated by electron, photon, or ion irradiation occurs within an ultrashort time scale of femtoseconds, while the bond breakage occurs within a sub-picosecond time scale, the excited state has to be sufficiently long lived so that the desorption product can gain a large kinetic energy to allow the chemical-bond scission to occur and the ionic product to survive from its image potential. Moreover, whether the desorption products leave the surface as neutrals or ions should be further determined by the neutralization process of the desorbing ions. It is in terms of these considerations that very recently, Souda and co-workers have claimed that the ion-stimulated O<sup>+</sup> and F<sup>+</sup> desorption is not initiated by the valence holes but rather caused by the formation of a (semi)core-hole state having the antibonding character.<sup>16–22</sup>

We now turn to the dynamics of CN<sup>-</sup> desorption as observed in the present work. Because of the chemical inertness of *RG* atoms, the CN<sup>-</sup> desorption should be attributed to either the translational energy or the potential energy carried by the incident *RG* ions or both. As the ion fluence is in a range of  $\sim 10^{13}$  ions/cm<sup>2</sup> s and the timescale of ion desorption is  $10^{-13}$ – $10^{-14}$  s, the CN<sup>-</sup> desorption should be a result of a single collision rather than consecutive collision events. This is also supported by the strong correlation between the product MTE and the incident ion energy. Consequently, the kinetic sputtering or collision-induced desorption mechanism is excluded because it cannot account for the energy origin of the CN<sup>-</sup> product in the low incident energy range. Thus, the potential energy carried by the incident *RG* ion was partly converted into the product translational energy, suggesting that the hole of the incident *RG* ion played an important role in initiating CN<sup>-</sup> desorption.

When a slow *RG* ion approaches the surface, it either survives from the interaction (and is then scattered away from the surface) or is neutralized by an electron from the surface. The former process transfers only part of its translational energy to the surface which is not sufficient to initiate the desorption event in the low incident energy range as mentioned above. Hence, the latter is believed to be responsible for the CN<sup>-</sup> desorption. In most cases, the neutralization occurs via resonant or Auger electron transfer processes with delocalized surface valence electrons, which, however, results in no CN<sup>-</sup> desorption. Thereby, the CN<sup>-</sup> emission must result from a localized interaction between the incident ion and a surface CN species. Furthermore, the fact that the

CN<sup>-</sup> MTE under 0-eV *RG* ion irradiation is independent of the *RG* ion species suggests that the CN<sup>-</sup> ion originates from an identical excited state that is produced by the localized interaction but independent of the *RG* ion species. Because both the 2*s* and 2*p* orbitals of the C and N atoms of chemisorbed CN species are hybridized to form molecular orbitals as schematically illustrated in Fig. 5, whereas the potential energies of the *RG* ions are small relative to the C or N 1*s* level, the nature of the localized interaction would be resonant and/or Auger neutralization of the *RG* ions by bonding or nonbonding electrons from these molecular orbitals. This leads to the formation of one or two holes (Auger decay) at the molecular orbital(s).

The conventional Auger desorption model (KF or AD model) would suggest that localized interatomic Auger decay of an incident *RG* ion ejects the two bonding electrons from the molecular orbital of the surface-CN bond [IV in Fig. 5(a)]. This leads to spontaneous disintegration of the bond and causes violent repulsion between the bonding atoms, which results in the decomposition of energetic CN and/or CN<sup>+</sup> particles from the surface. In this framework, however, the CN<sup>-</sup> yield dependence on *RG* ion species is expected in an order of He<sup>+</sup> > Ne<sup>+</sup> > Ar<sup>+</sup>, against the results of Fig. 1. On the other hand, the AD model also suggests desorption of CN<sup>+</sup> ions, which was not observed in the present experiments.

Instead, we attribute the initiating event of CN<sup>-</sup> desorption to a localized resonant or quasi-resonant electron exchange between an incident *RG* ion and a surface CN species, which creates a hole at a molecular orbital of chemisorbed CN species (Fig. 5). The quasis resonant electron exchange is possible between an incident ion and a target atom provided that they are located energetically within  $\pm 5$  eV.<sup>32,33</sup> Creation and localization of a hole at a molecular orbital pushes it to a high and repulsive potential surface (Franck-Condon transition), subsequent decay of the excited state may convert part of the potential energy to the translational energy of the surface CN and result in ejection of CN and/or CN<sup>+</sup> from the surface. The ejected CN species capture electrons from the surface via resonant process to form ultimately CN<sup>-</sup> ions. This is understood within the framework of the MGR model,<sup>2,3</sup> and accounts for the high CN<sup>-</sup> MTE and its independence of the *RG* ion species at 0-eV incident energy. In this respect, the dependence of the CN<sup>-</sup> yield on the *RG* ion species may partly reflect the energetic accessibility of the molecular orbital to the *RG* ion's hole to enable the (quasi)resonant electron exchange process [see Fig. 5(b)].

Furthermore, if a hole is created within the surface-CN bonding orbital by either resonant or Auger neutralization, the excitation should dissipate rapidly on a wide-band surface such as graphite. Whether or not this results in desorption is under debate.<sup>17–22</sup> In this respect, from the chemical point of view, the bonding electrons of the C $\equiv$ N bond [I and II in Fig. 5(a)] are spatially more localized than that of the surface-CN bond. As a consequence, a hole created at these orbitals may possess a longer lifetime to allow the bond scission to occur, and probably, is the initiating event of CN<sup>-</sup> desorption. More favorable is a hole created at the nonbond-

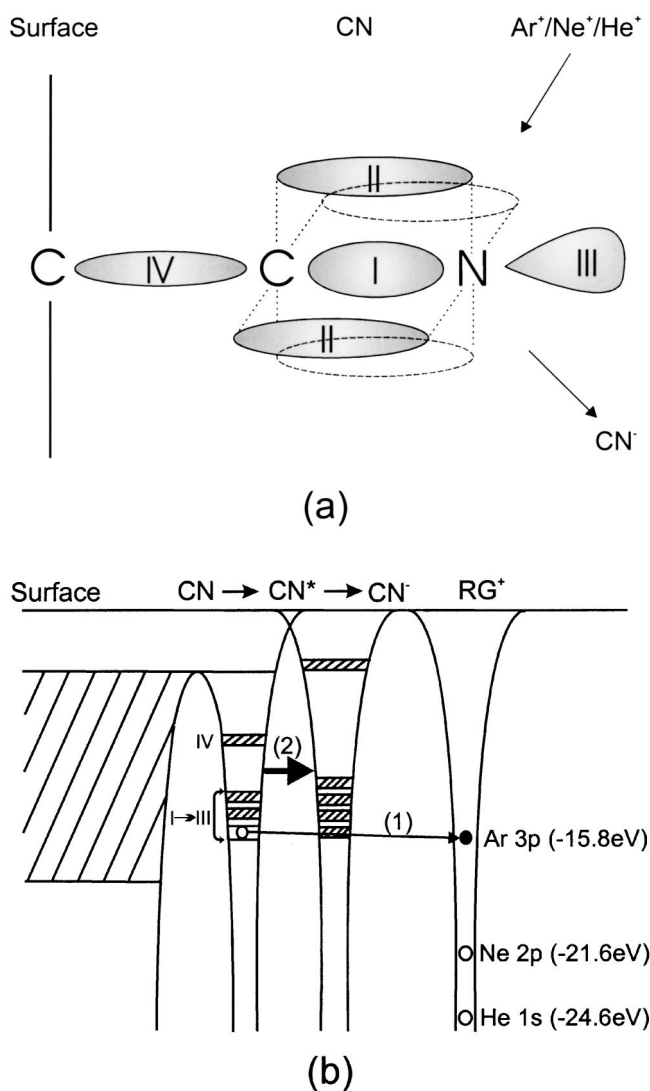


FIG. 5. (a) Schematic bonding and nonbonding molecular orbitals of chemisorbed CN at a graphite surface. The orbitals include one  $\sigma$  bond (I) and two  $\pi$  bonds (II) between C and N atoms (C $\equiv$ N bond), a nonbonding orbital localized at the N atom (III) and a chemisorptive bond between CN and the surface (surface-CN bond) (IV). All these orbitals are occupied. The energy diagram involved in the CN<sup>-</sup> formation is illustrated in (b): The chemisorptive bond orbital (IV) may merge into the valence band orbitals of graphite, but the C $\equiv$ N bond and the nonbonding orbitals (I–III) are more localized. The energy levels of these orbitals can be as deep as the first ionization potential of CN (13.6 eV) or even deeper, so that the quasisonant process is energetically allowable. As a result, neutralization of an incident RG ion creates a hole localized at a bonding or nonbonding orbital of chemisorbed CN. A subsequent decay of the excited state imparts kinetic energy into surface CN, and results in the ejection of CN from the surface. Negative ionization occurs during its departure from the surface, ultimately yielding a CN<sup>-</sup> ion.

ing orbital localized at N atom [III in Fig. 5(a)], which is screened spatially from access to surface electrons provided that the CN is adsorbed vertically to the surface. Nevertheless, the subsequent bond scission occurs at the weak

surface-CN chemisorptive bond rather than the much stronger C $\equiv$ N bond, leading to the ejection of CN particles from the surface. In reality, the hole need not necessarily be located at the bond to be broken as also demonstrated by the desorption of O<sup>+</sup> and F<sup>+</sup> ions.<sup>16–22</sup> During or after the bond breakage, the CN electronic structure experiences a rearrangement, which allows access of the desorbing CN to the surface electrons, so that negative ionization may occur.

Negative ionization of CN at graphite surface is further facilitated by the band effect.<sup>34</sup> Graphite is a semimetal with 0-eV band gap, and its valence band extends from its Fermi level down to  $\sim 22$  eV below the vacuum level. The surface work function of the nitrogenated graphite surface is determined to be  $\sim 4.06$  eV.<sup>30</sup> The positive ionization potential of CN is  $\sim 13.6$  eV, and its affinity level is  $\sim 3.86$  eV below the vacuum level.<sup>35</sup> Since the CN particles are created at the surface, both the ionization and the affinity levels will shift near to but below the surface Fermi level upon departure. Consequently, negative ionization of a desorbing CN can readily occur via a resonant process. Meanwhile, the resulting CN<sup>-</sup> ion can survive from reneutralization in a large probability due to the small energy difference of the CN<sup>-</sup> affinity level relative to the top of the valence band ( $\sim 0.2$  eV). A facile and dominant negative ionization of CN also occurs during carbon atom abstraction by hyperthermal N<sup>+</sup> ions<sup>27</sup> and nitrogen ion sputtering of graphite.<sup>28</sup> In this respect, the absence of CN<sup>+</sup> desorption is ascribed to (i) the electronic structure of a desorbing CN particle which favors negative ionization, and (ii) the absence of a CN (semi-)core-level accessible to the RG ions.

In the frame of the above mechanism, we should have observed CN<sup>-</sup> ions originating from both potential desorption and direct carbon abstraction during hyperthermal N<sup>+</sup> ion irradiation of graphite. In order to clarify this point, a nitrogenated graphite sample was also subjected to 2–30-eV N<sup>+</sup> ion irradiation. We indeed observed emission of CN<sup>-</sup> ions with maximum energy close to that produced by RG ion irradiation. Hence, the insignificance of a potential desorption of the CN<sup>-</sup> ion during N<sup>+</sup> irradiation of fresh graphite is partly due to a low surface CN population, which accounts for the large CN<sup>-</sup> MTE difference between 0-eV RG ion irradiation and N<sup>+</sup> abstraction, as shown in Fig. 4.

## V. SUMMARY

In summary, we have shown that hyperthermal RG ion irradiation efficiently induces CN<sup>-</sup> desorption from a nitrogenated graphite surface. The translational energy obtained by the CN<sup>-</sup> ions during very low energy RG ion irradiation is relatively high in comparison with the incident energy. It is proposed that the CN<sup>-</sup> emission occurs as a result of potential-stimulated desorption. The initiating event is the formation of a localized hole at a bonding or nonbonding molecular orbital of chemisorbed CN species by resonant or quasisonant neutralization of incident RG ion. A subsequent decay of the excited state results in the ejection of energetic CN species from the surface, which capture electrons from the surface via a resonant process to form ultimately CN<sup>-</sup> ions.

- \*Corresponding author. Present address: Ion Reaction Laboratory, Department of Nuclear Medicine and Radiobiology, Faculty of Medicine, University of Sherbrooke, Sherbrooke, Quebec, J1H 5N4, Canada. FAX: (1)-819-564-5442. Electronic mail: dengzw@yahoo.com
- <sup>†</sup>Electronic mail: SOUDA.Ryutaro@nims.go.jp
- <sup>1</sup>R. D. Ramsier and J. T. Yates, Jr., *Surf. Sci. Rep.* **12**, 243 (1991).
- <sup>2</sup>D. Menzel and R. Gomer, *J. Chem. Phys.* **41**, 3311 (1964).
- <sup>3</sup>P. Redhead, *Can. J. Phys.* **42**, 886 (1964).
- <sup>4</sup>M. L. Knotek and P. Feibelman, *Phys. Rev. Lett.* **40**, 964 (1978).
- <sup>5</sup>R. Franchy and D. Menzel, *Phys. Rev. Lett.* **43**, 865 (1979).
- <sup>6</sup>D. P. Jennison, J. A. Kelber, and R. R. Rye, *Phys. Rev. B* **25**, 1384 (1982).
- <sup>7</sup>D. E. Ramaker, C. T. White, and J. S. Murday, *Phys. Lett.* **89A**, 211 (1982).
- <sup>8</sup>H. H. Madden, D. R. Jennison, M. M. Traum, G. Margaritondo, and N. G. Stoffel, *Phys. Rev. B* **26**, 896 (1982).
- <sup>9</sup>D. R. Jennison and D. Emin, *Phys. Rev. Lett.* **51**, 1390 (1983).
- <sup>10</sup>K. Wittmaak, *Phys. Rev. Lett.* **43**, 872 (1979).
- <sup>11</sup>P. Williams, *Phys. Rev. B* **23**, 6187 (1981).
- <sup>12</sup>P. Varga, U. Diebold and D. Wutte, *Nucl. Instrum. Methods Phys. Res. B* **58**, 417 (1991).
- <sup>13</sup>J. Lorincik, Z. Sroubek, and H. Gnaser, *Surf. Sci.* **314**, 373 (1994).
- <sup>14</sup>Z. Sroubek and H. Oechsner, *Surf. Sci.* **311**, 263 (1994).
- <sup>15</sup>M. Petravic and J. S. Williams, *Nucl. Instrum. Methods Phys. Res. B* **101**, 64 (1995).
- <sup>16</sup>R. Souda, *Phys. Rev. Lett.* **82**, 1570 (1999).
- <sup>17</sup>R. Souda, *Phys. Rev. B* **60**, 6068 (1999).
- <sup>18</sup>R. Souda, T. Suzuki, E. Asari, and H. Kawanowa, *Phys. Rev. B* **60**, 13 854 (1999).
- <sup>19</sup>R. Souda, H. Kawanowa, S. Otani, and T. Aizawa, *Phys. Rev. B* **60**, 14 412 (1999).
- <sup>20</sup>R. Souda, H. Kawanowa, S. Otani, and T. Aizawa, *J. Chem. Phys.* **112**, 979 (2000).
- <sup>21</sup>R. Souda, S. Otani, and H. Kawanowa, *J. Phys. Chem. B* **104**, 5492 (2000).
- <sup>22</sup>R. Souda, *Int. J. Mod. Phys. B* **14**, 1139 (2000).
- <sup>23</sup>G. Hayderer, M. Schmid, P. Varga, H. P. Winter, F. Aumayr, L. Wirtz, C. Lemell, J. Burgdorfer, L. Hagg, and C. O. Reinhold, *Phys. Rev. Lett.* **83**, 3948 (1999).
- <sup>24</sup>M. Maazouz, T. L. O. Barstis, P. L. Maazouz, and D. C. Jacobs, *Phys. Rev. Lett.* **84**, 1331 (2000).
- <sup>25</sup>C. L. Quinteros, T. Tzvetkov, and D. C. Jacobs, *J. Chem. Phys.* **113**, 5119 (2000).
- <sup>26</sup>M. Kurahashi and Y. Yamauchi, *Phys. Rev. Lett.* **84**, 4725 (2000).
- <sup>27</sup>Z.-W. Deng and R. Souda, *J. Chem. Phys.* **117**, 6235 (2002).
- <sup>28</sup>Z. W. Deng and R. Souda, *Nucl. Instrum. Methods Phys. Res. B* **183**, 260 (2001).
- <sup>29</sup>Z. W. Deng and R. Souda, *Thin Solid Films* **406**, 46 (2002).
- <sup>30</sup>Z. W. Deng and R. Souda, *J. Chem. Phys.* **116**, 1725 (2002).
- <sup>31</sup>J. I. Gersten and N. Tzoar, *Phys. Rev. B* **16**, 945 (1977).
- <sup>32</sup>T. W. Rusch and R. L. Erickson, *J. Vac. Sci. Technol.* **13**, 374 (1976).
- <sup>33</sup>A. Zartner, E. Taglauer, and W. Heiland, *Phys. Rev. Lett.* **40**, 1259 (1978).
- <sup>34</sup>S. Tsuneyuki, N. Shima, and M. Tsukada, *Surf. Sci.* **186**, 26 (1987).
- <sup>35</sup>*CRC Handbook of Chemistry and Physics*, edited by D. R. Lide (CRC Press, New York, 2001).